Topics in Catalysis Vol. 39, Nos. 3–4, October 2006 (© 2006)
DOI: 10.1007/s11244-006-0055-0

Novel, uniform nanostructured catalytic membranes

P.C. Stair[a,b,*], C. Marshall[d], G. Xiong[c], H. Feng[a], M.J. Pellin[c], J.W. Elam[e], L. Curtiss[b], L. Iton[c], H. Kung[f], M. Kung[f], and H.-H. Wang[c]

[a]*Department of Chemistry and Center for Catalysis and Surface Science, Northwestern University, Evanston, IL 60208, USA*
[b]*Chemistry Division, Argonne National Laboratory, Argonne, IL 60439, USA*
[c]*Materials Science Division, Argonne National Laboratory, Argonne, IL 60439, USA*
[d]*Chemical Engineering Division, Argonne National Laboratory, Argonne, IL 60439, USA*
[e]*Energy Systems Division, Argonne National Laboratory, Argonne, IL 60439, USA*
[f]*Chemical Engineering Department, Northwestern University, Evanston, IL 60208, USA*

Nanostructured membrane structures have been fabricated by a combination of anodic aluminum oxidation (AAO) and atomic layer deposition (ALD) for use as platforms for the synthesis of highly uniform heterogeneous catalysts. The ALD method makes it possible to control pore diameters on the Angstrom scale even when the overall pore diameter is 10's to 100's of nanometers. AAO membranes imbedded in an aluminum sealing ring have been tested for flow properties and found to follow Knudsen diffusion behavior. Vanadia-coated membranes have been tested for the catalytic oxidative dehydrogenation of cyclohexane and show improved selectivity at the same conversion compared to conventional powdered alumina supported vanadia catalysts.

KEY WORDS: nanostructured membranes; anodic aluminum oxidation (AAO); atomic layer deposition (ALD).

1. Introduction

The functionality of a heterogeneous catalyst depends critically on its structure over a range of length scales [1]. Thus, development of synthetic methods to control the atomic structure of both the active site and its associated supporting framework would make possible the manipulation of catalyst performance by influencing the rates and selectivity of catalytic chemical reactions. An important example of the role played by atomic scale framework control is the molecule shape selectivity exhibited by catalysts based on the microporous nature of zeolites [2,3]. At the somewhat longer length scale of (10's to 1000's of nanometers), the dimensions and topology of the catalyst pore structure can influence reagent flow, the sequencing of catalytic active sites, and the contact time between reagents and catalyst [4].

A particularly interesting concept for a catalyst topology is the nanostructured membrane pictured in figure 1. Conceptually, the membrane consists of an assembly of identical pores having nanometer dimensions that span a flow reactor so as to produce an array of nanoreactors. With this assembly, each reagent molecule must traverse an identical pore and, ideally, each diffusion path can be engineered through control over the pore diameter, wall composition, and length. This results in more uniform (and controllable) contact times than are possible with a conventional fixed bed catalyst. Moreover, if the pore diameter could be adjusted to atomic dimensions, then reagent-size control similar to a zeolite would be possible. By coating the pore walls one might imagine exercising control over reagent flow through hydrophilic or hydrophobic interactions as shown in the bottom of figure 1. In principle, this chemical gradient might be used to enhance the removal of products, reducing the probability of additional (unwanted) reactions. With a sufficiently large number of pores in the array, it might be possible to form one catalytically active particle in each pore and still have enough catalytic material for practical applications or fundamental studies. If only one particle resides in each pore, then sintering would be virtually eliminated. Finally, since reagents flow preferentially in one direction through this structure, there exists the potential to sequence different catalytic sites along each pore.

*To whom correspondence should be addressed.
E-mail: pstair@northwestern.edu

2. Uniform, nanostructured membranes

Nanostructured membrane frameworks that approach the ideal characteristics described above have been fabricated at Argonne National Laboratory and Northwestern University using a combination of anodic aluminum oxidation (AAO) and atomic layer deposition (ALD) [5,6]. AAO membranes are an ideal scaffold with highly aligned, parallel pores and narrow pore-diameter distributions. Electrochemical conditions can be arranged to produce most probable pore diameters in the range 20–400 nm [7–12] and membrane thicknesses in the range 0.5 to >250 μm. For this work, highly-ordered, 70 μm thick AAO scaffolds produced in oxalic acid [8,9] are used, containing pores with a most

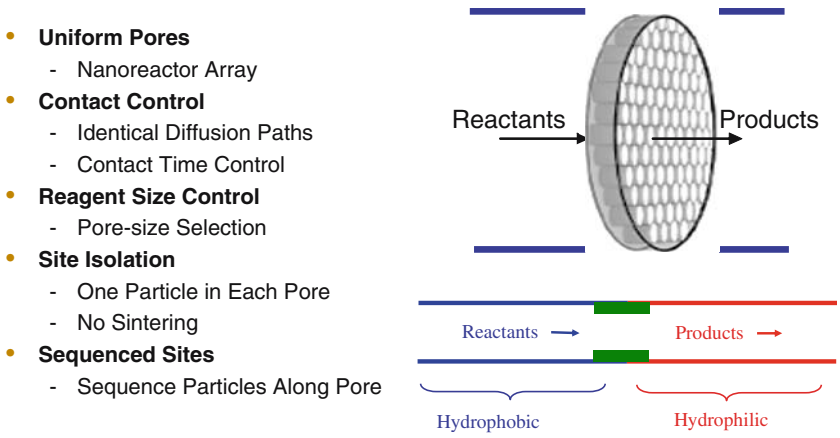

Figure 1. Schematic diagram of a nanostructured membrane catalyst topology.

probable diameter of 40 nm. The experimental details of their fabrication have been described previously [6]. Figure 2 shows an SEM plan view micrograph of an AAO membrane with 100 nm diameter pores made in 0.3 M oxalic acid. Note the uniform dimensions and hexagonal pore arrangement.

For applications in catalysis the as-grown membranes suffer from poorly defined pore wall morphology and composition with significant (5%) amounts of incorporated electrolyte anions [6, 13, 14]. ALD was used to precisely control the chemical composition and diameters of the AAO scaffold pores. ALD is a growth technique that uses alternating, saturating reactions between gaseous precursor molecules and a substrate to deposit films in a layer-by-layer fashion [15]. By repeating the binary reaction sequence in an ABAB... fashion, films of micrometer thickness can be deposited with atomic layer precision. Binary reaction sequences have been developed to deposit a wide variety of materials including oxides, nitrides, sulfides and metals [16]. Because gas transport into mesoporous and microporous materials is diffusion-limited; surfaces at the entrance to the AAO membrane will receive reactant exposures that are $\sim 10^3$ larger than the interior surface. Despite this, ALD has a demonstrated ability to coat mesoporous materials uniformly [17, 18] including AAO [19]. An example of pore diameter control and uniformity with ALD coated AAO is depicted in figure 3.

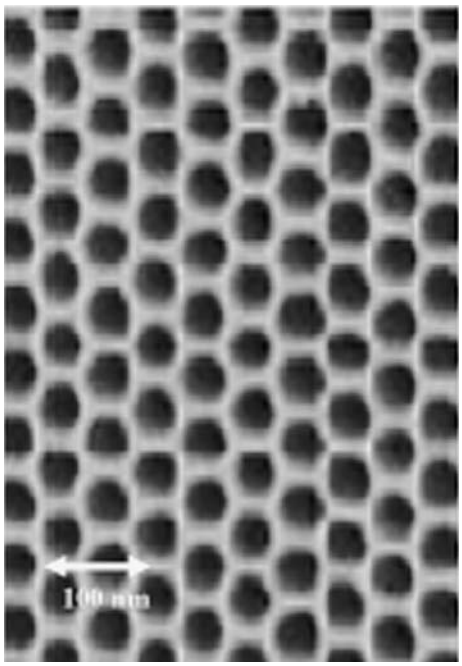

Figure 2. SEM plan view of a uniform array of pores grown using 0.3 M oxalic acid. Each pore is approximately 40 nm in diameter.

The AAO + ALD nanostructured membranes are fragile objects, easily cracked and difficult to handle. In order to overcome these mechanical shortcomings and to provide a surface for sealing the membranes into a flow reactor, a procedure for growing the membranes in the center of an aluminum ring has been developed. Essentially, aluminum foil, which is the starting point for producing AAO, is cut into the shape of a disk. With appropriate masking of the disk's perimeter, to prevent contact with the electrolyte used to oxidize the aluminum, a ring of metal is preserved that can be used for handling and sealing (see figure 4).

3. Flow and catalytic studies

Gas conductance measurements were performed on AAO's imbedded in aluminum rings in order to evaluate the effectiveness of sealing into a standard VCR fitting and to investigate the reproducibility and uniformity of the AAO pore structure. The apparatus for gas conductance measurements is shown schematically in figure 5. Conductance, C, is given by the equation $C = Q/(P_1–P_0)$, where Q is the gas flow rate setting of the mass flow controller (MFC), either 20 or 200 sccm full scale, P_0 is the pressure reading on the Baratron gauge at this flow with no membrane in place, and P_1 is the pressure measured with the membrane sealed in a VCR fitting before the vent. Figure 6 shows the

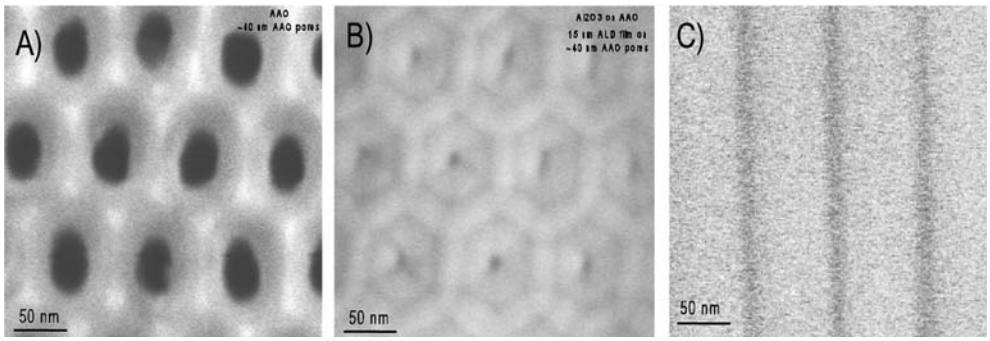

Figure 3. (A) Plan view SEM image of surface of the original 40 nm AAO material. (B) Plan view SEM image of the surface of the 40 nm AAO material coated with 15 nm of alumina. (C) Cross sectional view of 40 nm AAO material coated with 15 nm of alumina taken from the center of the AAO membrane (note that the coating is uniform despite the high aspect ratio).

Figure 4. Photograph of an AAO membrane surrounded by an aluminum ring. The slight refraction of the grid lines in the center of the aluminum ring indicates the presence of the AAO membrane.

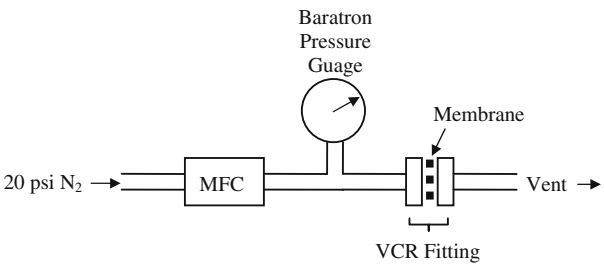

Figure 5. Apparatus for gas conductance measurements of AAO membranes embedded in Al-ring. MFC = mass flow controller. The Baratron pressure gauge has 1500 torr full-scale reading.

measured Q versus ΔP for three different membranes with nominal pore diameters of 40 nm determined from SEM micrographs. The excellent linearity and reproducibility of the data for the three membranes is consistent with highly uniform structures. For pore diameters less than 50 nm the gas flow is governed by Knudsen diffusion [4]. Using the geometric thickness of the membrane and the pore density from SEM images, the pore diameter calculated from the Knudsen equation and the measured gas flow conductance is 43 ± 1 nm.

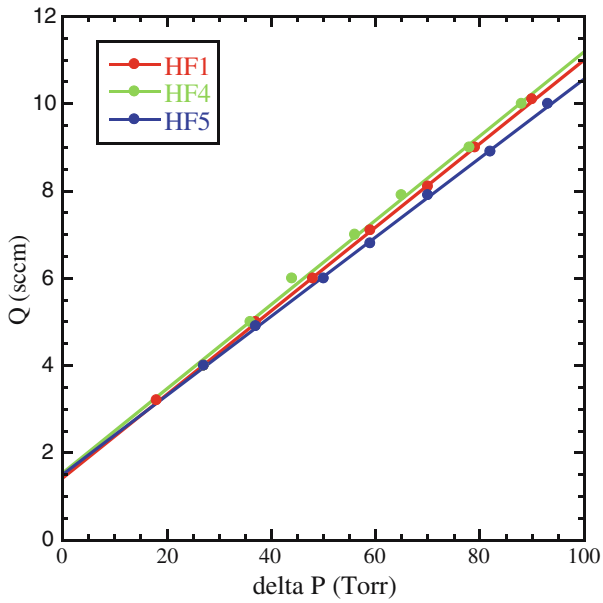

Figure 6. Gas flow rate versus pressure change across three different membranes.

The excellent agreement between this value and the nominal 40 nm diameter (measured from SEM images) is strong support for Knudsen diffusion and indicates that the gas flow is not determined by cracks or other imperfections.

The effect of reducing the pore diameter by ALD of aluminum oxide is shown in figure 7. In principle, each AB cycle of aluminum oxide ALD lays down one monolayer. The number of monolayers deposited is linear in the number of AB cycles. Figure 7A shows the reduced flow rate produced in a series of membranes after a number of AB cycles in the range 0–138 cycles. Notice the progressive reduction in the slopes of the linear Q versus ΔP curves which reflects the progressively smaller conductance through the membrane pores. The change in the y-axis intercept apparent for the curves obtained following 118 and 138 cycles is due to the different MFC used for these measurements.

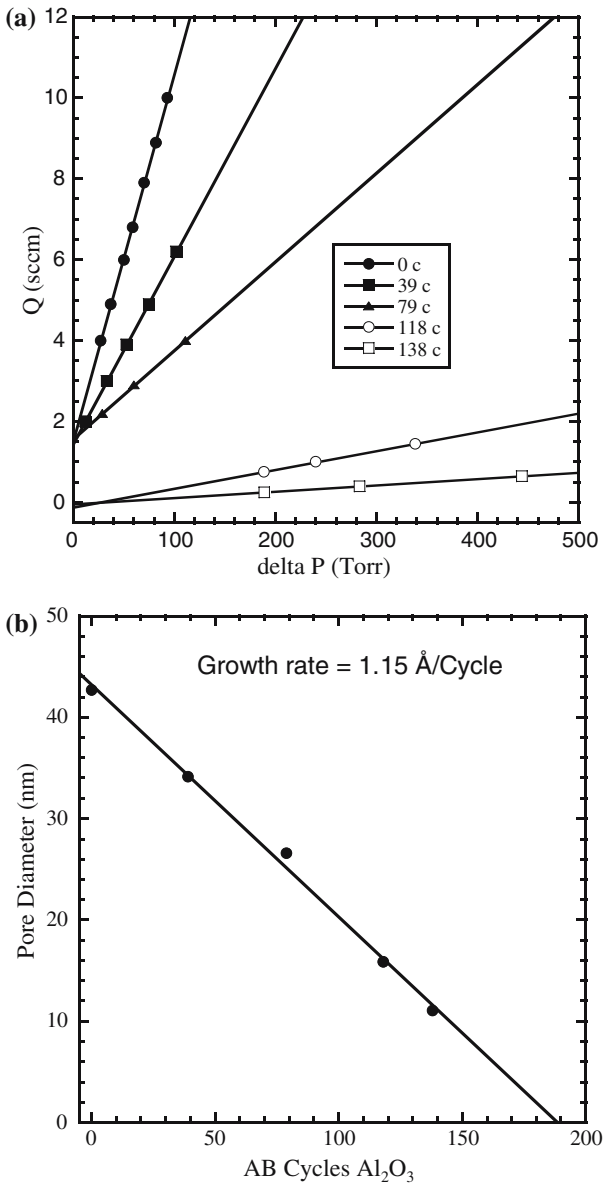

Figure 7. Conductance measurements on AAO membranes after pore diameter narrowing by ALD of alumina. (A) Flow versus ΔP for membranes following 0–138 AB cycles of $A1_2O_3$ deposition. (B) Pore diameter determined by the measured conductance versus the number of AB cycles.

Application of the Knudsen equation to the conductance determined from the flow measurements is used to derive a value for the average pore diameter. A plot of the pore diameter versus the number of AB cycles is highly linear as seen in figure 7B. The slope of this plot indicates that each AB cycle of aluminum oxide deposition reduces the pore diameter by 1.15 Å. This demonstrates that ALD is capable of controlling pore diameter at the atomic scale even when the overall diameter is at the scale of 10's to 100's of nanometers.

To test the activity and selectivity changes in moving from a standard powdered catalyst to membrane mounted catalysts, catalytic tests for oxidative dehydrogenation (ODH) were run for V_2O_5 coated AAO materials and for gamma alumina coated with V_2O_5. The reactor was a simple plug flow design in an up flow configuration (see figure 8). In the case of the AAO membranes, bypass of the membrane was minimized but could not be eliminated. Measured activities should therefore be considered as lower limits.

Figure 9 shows the activity and selectivity for ODH of cyclohexane over V_2O_5 on alumina at 1% and 20% compared to a membrane. The membrane was prepared by first depositing 10 nm of alumina by ALD into an AAO with 40 nm pores. Finally, vanadia was deposited by wet impregnation to 1 monolayer coverage using ammonium metavanadate. At the given temperature (450 °C) the conversions are nearly identical (4% for the 1% V_2O_5/alumina versus 5% for the V_2O_5/AAO). The conversion of the 20% V_2O_5 on alumina is much higher at 17%. In all cases, the selectivity for the AAO coated material is very different from the powder catalysts. The AAO material is more selective to cyclohexene (25 versus 15%) and benzene (28 versus 8%) than 1% V_2O_5 on powder alumina. Selectivity for the deep oxidation products (CO and CO_2) are lower for the AAO material (CO = 12% for AAO versus 19% for the 1% V_2O_5 on alumina and CO_2 = 31% versus 55% for AAO and 1% V_2O_5 on alumina). As can be seen in figure 9, the AAO membrane shows a similar selectivity improvement over the 20% V_2O_5 on alumina.

Figure 10 compares the activity of a 1 nm alumina-coated membrane with and without V_2O_5 added. As can be seen from this plot, the activity of the AAO catalyst is purely from the V_2O_5 coating. No ODH activity is observed for the material containing only $A1_2O_3$ in the pores. The activity with V_2O_5 coating increases monotonically with increasing temperature.

Figure 11 shows the changes in the selectivity of the vanadium-coated AAO as a function of the pore size of the AAO material. The smaller pore AAO was produced by coating an AAO membrane with 10 nm of alumina before wet impregnation of the pores with vanadia. The smaller pore membrane shows greater selectivity to cyclohexene and lower selectivity to both CO and CO_2. The benzene yield for each material is nearly the same.

The vanadia-coated AAO-supported ALD membranes, especially the one with 10 nm channels, show higher selectivity than the conventional catalysts. The improved selectivity for the AAO catalysts may reflect a limiting of secondary oxidation reactions by a contact time of the reagents which is 10^3–10^4 times shorter in the membrane channels than in the conventional catalyst bed. The uniform pore diameter may result from the uniformity of the $A1_2O_3$ ALD coating leading to extremely monolithic pore diameters and pore wall compositions. While the conversion percentages for O_2 and C_6H_{12} are lower for the 10 nm membrane than its larger pore cousins, the conversion per mole of vana-

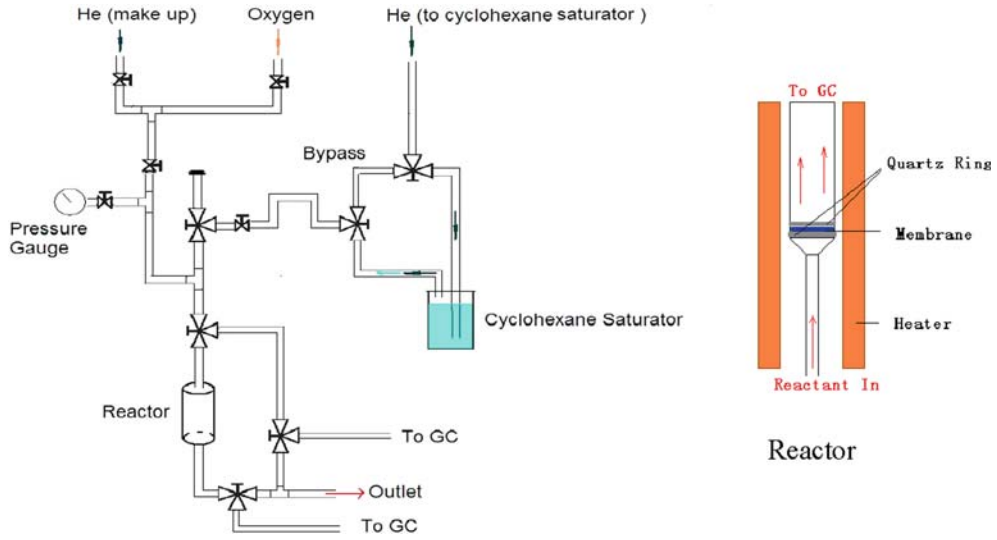

Figure 8. Flow system and reactor for membrane catalysis experiments. The unmounted membranes are sandwiched between two quartz rings in a quartz flow tube.

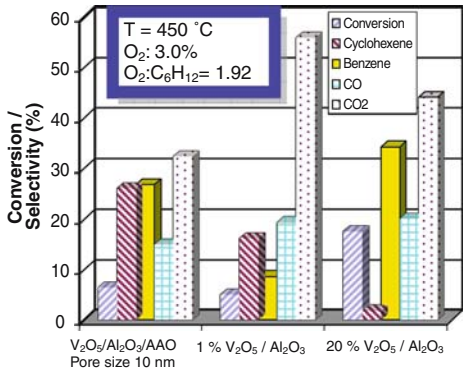

Figure 9. Activity and selectivity comparison for oxidative dehydrogenation of cyclohexane over V_2O_5 on alumina versus on AAO.

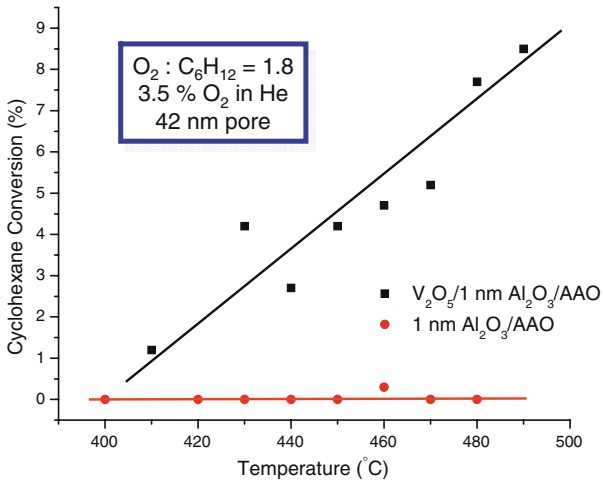

Figure 10. ODH conversion for cyclohexane for a V2O5-coated AAO membrane versus the corresponding membrane without V2O5 coating. Each AAO membrane has a 1 nm coating of alumina.

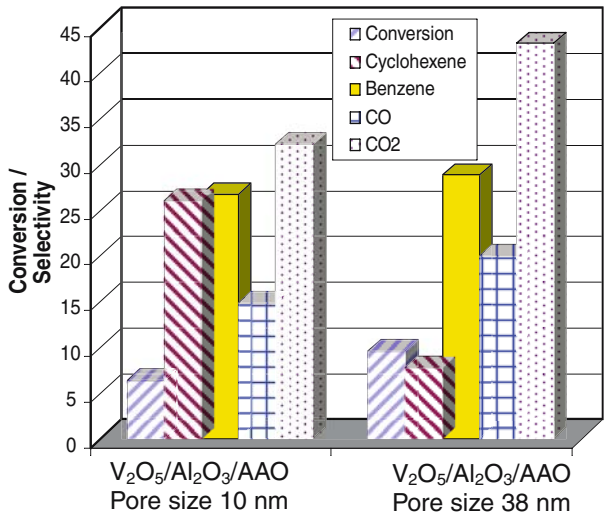

Figure 11. Activity/Selectivity for cyclohexane conversion for a V_2O_5 coated on two different pore diameters (10 and 38 nm) of AAO membrane.

date is significantly higher. Part of the reason for this is the increase in wall collisions associated with the smaller pore diameter. Further, since the mean free paths of molecules under these conditions are 50 nm, the molecular flux in the larger channels may be a combination of convective and Knudsen flow. The velocity profile of convective flow would be laminar in which the flow in the center is proportionately over-collected when sampling at the exit. Essentially, this portion of the sample bypasses the reactor without contact with the catalyst on the wall. There is also a significant and repeatable difference in selectivity between 10 nm ALD pores and 38 nm pores. The 10 nm pores are more selective to the desirable cyclohexene and less selective to the less desirable deep

oxidation products (CO and CO_2). We are currently investigating the cause of this difference, which may result from changes in pore wall electronic structure or from flow dynamics.

Acknowledgments

The work at Argonne is supported by the U.S. Department of Energy, BES-Materials Sciences (materials synthesis), and BES-Chemical Sciences (catalytic activity) under Contract W-31-109-ENG-38. The work at Northwestern is supported by the U.S. Department of Energy, BES-Chemical Sciences, Geosciences and Biosciences Division under Grant No. DE-FG0203ER15457.

References

[1] J.G. Goodwin Jr., S Kim and W.D. Rhodes, Catalysis 17 (2004) 320.
[2] J. Weitkamp, S. Ernst, and L. Puppe, in: *Catalysis and Zeolites*, eds. J. Weitkamp and L. Puppe (Springer, Berlin, 1999) p. 327.
[3] E. Klemm, H. Seiler, G. Emig G. A computer simulation of shape selective catalysis on zeolites. Stud. Surf. Sci. Catal. 98 (Zeolite Science 1994: Recent Progress and Discussions) (1995) 246.
[4] S. Roy, R. Raju, H.F. Chuang, B.A. Cruden and M. Meyyappan, J. Appl. Phys. 93(8) (2003) 4870.
[5] M.J. Pellin, P.C. Stair, G. Xiong, J.W. Elam, J. Birrell, L. Curtiss, S.M. George, C.Y. Han, L. Iton, H. Kung, M. Kung and H.H. Wang, Catal. Lett. 102(3–4) (2005) 127.
[6] G. Xiong, J.W. Elam, H. Feng, C. Y. Han, H.-H. Wang, L.E. Iton, L.A. Curtiss, M.J. Pellin, M. Kung, H. Kung and P.C. Stair, J. Phys. Chem. B 109(29) (2005) 14059.
[7] G.D. Bengough and J.M. Stuart, Br. Patent 223 (1923) 994.
[8] C.Y. Han, Z.L. Xiao, H.H. Wang, G.A. Willing, U. Geiser, U. Welp, W.K. Kwok, S.D. Bader and G.W. Crabtree, ATB Metall. 43(1–2) (2003) 123.
[9] C.Y. Han, Z.L. Xiao, H.H. Wang, G.A. Willing, U. Geiser, U. Welp, W.K. Kwok, S.D. Bader, and G.W. Crabtree, Anodized aluminum oxide membranes as templates for nanoscale structures. *Proceedings – AESF. SUR/FINAnnual International Technical Conference* (2003), 128.
[10] H. Masuda and Fukuda, Science (Washington, D. C.) 268(5216) (1995) 1466.
[11] V.P. Menon and C.R. Martin, Anal. Chem. 67 (1995) 1920.
[12] K.N. Rai and E. Ruckenstein, J. Catal. 40(1) (1975) 117.
[13] G. Patermarakis and K. Moussoutzanis, Corrosion Sci. 44(8) (2002) 1737.
[14] G. Patermarakis, K. Moussoutzanis and Nikolopoulos, J. Solid State Electrochem. 3(4) (1999) 193.
[15] S.M. George, A.W. Ott and J.W. Klaus, J. Phys. Chem. 100 (1996) 13121.
[16] M. Ritala and M. Leskela, in: *Handbook of Thin Film Materials*, Vol. 1, ed. H.S. Nalwa, (Academic Press, San Diego, 2001).
[17] M.A. Cameron, I.P. Gartland, J.A. Smith, S.F. Diaz and S.M. George, Langmuir 16(19) (2000) 7435.
[18] C.A. Cooper and Y.S. Lin, J. Memb. Sci. 195(1) (2002) 35–50.
[19] J.W. Elam, D. Routkevitch, P.P. Mardilovich and George, Chem. Mater. 15 (2003) 3507.